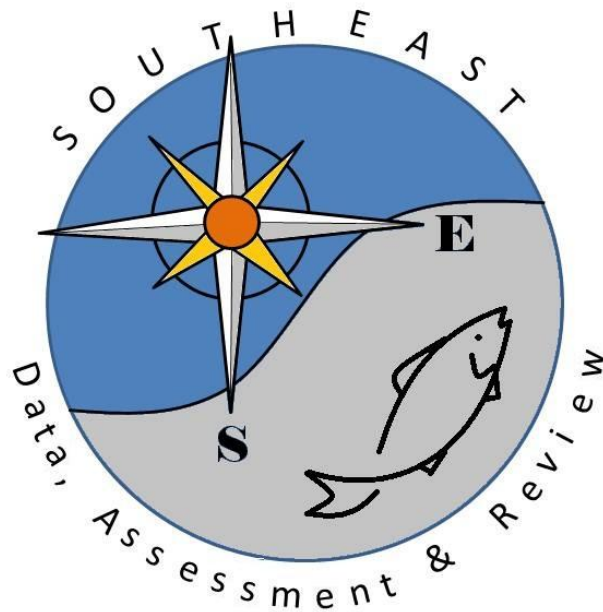


Modeling the dependence of batch fecundity and spawning frequency on size and age for use in stock assessments of red snapper in U.S. Gulf of Mexico waters

Clay E. Porch, Gary R. Fitzhugh, and Brian C. Linton

SEDAR31-AW03

11 January 2013



This information is distributed solely for the purpose of peer review. It does not represent and should not be construed to represent any agency determination or policy.

Please cite as:

Porch, C.E., G.R. Fitzhugh, and B.C. Linton. 2013. Modeling the dependence of batch fecundity and spawning frequency on size and age for use in stock assessments of red snapper in U.S. Gulf of Mexico waters. SEDAR31-AW03. SEDAR, North Charleston, SC. 22 pp.

Modeling the dependence of batch fecundity and spawning frequency on size and age for
use in stock assessments of red snapper in U.S. Gulf of Mexico waters

C.E. Porch¹, G.R. Fitzhugh², and B.C. Linton¹

¹Southeast Fisheries Science Center
Sustainable Fisheries Division
75 Virginia Beach Drive
Miami, FL 33149-1099

²Southeast Fisheries Science Center
Panama City Laboratory
3500 Delwood Beach Rd.
Panama City, FL 32408

Introduction

Many tropical and subtropical fishes exhibit indeterminate fecundity and spawn multiple times over an extended period that may last much of the year. Several studies have demonstrated that the number of eggs produced during a spawning event (batch fecundity) increases at a faster rate than weight with age or body length. Moreover, evidence is emerging that the frequency of spawning events also increases with age and body size (Fitzhugh et al. 2011). As a result, egg production in tropical and subtropical species is probably less correlated to mature (spawning) biomass than has been observed for species from higher latitudes (Lowerre-Barbieri et al. 2011a, Fitzhugh et al. 2012).

Batch fecundity and spawning frequency also are likely to vary during the course of the spawning season. This poses difficulties for developing the relationship between egg production and age or size because different relationships may be apparent depending on when reproductive samples are taken (Lowerre-Barbieri et al. 2011a). Enhanced awareness of data needs and new approaches to simplify data collection and reproductive processing are coming into place (Klibansky and Juanes 2008, Lowerre-Barbieri et al. 2011b), but modeling approaches often remain ad-hoc because key data are missing (Fitzhugh et al. 2012, Workshop on Modeling Protogynous Hermaphroditic Fishes, Aug 2012, Mid-Atlantic Fisheries Management Council). For example, few studies we know of have attempted to estimate fecundity with some accounting of size, season, and annual variation in spawning frequency (Laplante and Schultz 2007, Mehault et al. 2010, Cooper et al 2013).

Recent stock assessments of Gulf of Mexico red snapper, *Lutjanus campechanus*, modeled egg production as the product of batch fecundity and maturity at age (Porch 2004, Porch et al. 2007). However, Porch et al. (2007) suggested that there was a need to account for age and size-contrast in the number of annual spawns, which in turn is a function of spawning frequency and duration. In 2011, a congressionally supported supplemental survey was conducted Gulf-wide with red snapper as one of the target species (Campbell et al. 2012). As multiple vessels conducted the survey synoptically throughout the red snapper spawning season (April through October), a more spatially and temporally extensive survey of spawning occurred than has been possible in the past.

The objective of this paper was to utilize the new survey information for red snapper to update the batch fecundity models developed for the last SEDAR assessment and develop new models of the dependence of the number of spawns on the time of year. The influence of depth, region, and sampling gear was also explored.

Methods

Data

The data on proportions of females bearing spawning markers are accompanied by information on maximum total length (l), age (a), depth in meters (d), gear type (vertical line or longline), region (east or west of the Mississippi River), and time of year. In addition, the SEDAR 31 data workshop panel recommended updating the batch fecundity models used during SEDAR 7 (Porch 2004, Porch et al. 2007) to include 85 new records from several sources (Fitzhugh et al. 2012, Brown-Peterson et al. 2009, Cowan, et al. 2012, Kulaw 2012, and Szedlmayer et al. 2000).

Analyses of BF

The relationship between batch fecundity (BF) and total length (l) is typically modeled with the power function

$$(1) \quad BF = cl^b e^\varepsilon$$

where e^ε represents a multiplicative model error (in which case the parameters c and b are usually estimated by a linear regression of the logarithm of BF on the logarithm of l).

Porch et al (2007) showed that, if growth in length follows a von Bertalanffy function, then the relationship between BF and age should have the form

$$(2) \quad BF = c(1 - e^{-kt})^b + \varepsilon$$

where ε is a normal distributed error term with mean 0 and variance σ . They note that if fecundity were primarily a function of length, then equation (2) would not be expected to fit the observations of BF as well as equation (1) except in the unlikely event that the variation in growth among individuals is negligible. Conversely, if fecundity were primarily an increasing or asymptotic function of age, then equation (2) might be expected to fit the data better than equation (1).

Porch et al. (2007) demonstrated a statistically significant dome-shaped relationship between BF and age within size classes. However, a model that incorporated this interaction explained only slightly more of the total variation in BF ($r^2 = 45\%$) than the simple power function of length ($r^2 = 42\%$). Inasmuch as the available data on BF are essentially unchanged, we did not revisit this interaction further.

Analyses of spawning fraction

Fitzhugh et al. (2012) showed that the proportion of females bearing histological spawning markers (spawning fraction, p) increased asymptotically with both age and length, which suggests that a logistic regression might be appropriate. However, they also found that spawning fraction varied with the time of sampling, gradually increasing from April to a peak in July, and then decreasing back to negligible levels by late October. In as much as the sampling was not conducted uniformly for all depths, regions and gears throughout the year, it is possible that the relationship between spawning fraction and age or length could be confounded with seasonal variations in sampling. For example, since older red snapper tend to be caught in deeper water, sampling deep and shallow waters at different times of the spawning season could alter the apparent relationship between spawning fraction and age. Preliminary work has suggested that the gear used and region sampled may also affect the apparent spawning fraction. Accordingly, in order to develop an unbiased estimate of the relationship between p and age (or length), one must explicitly account for the effects of any factors that may have varied systematically during the sampling.

The spawning fraction at any given age (a), length (l) and time of year (t) may be written as the product

$$(3) \quad \begin{cases} p(a,t) = p(a)p(t|a) \\ p(l,t) = p(l)p(t|l) \end{cases} .$$

The relationship between spawning fraction and season can be modeled using the flexible gamma function:

$$(4) \quad p(t) = \left(\frac{t}{\mu} \right)^{\mu/K} e^{-(\mu-t)/K}$$

where t is the fraction of the year elapsed beginning on January 1, μ is the mode (time of peak spawning) and K is the dispersion coefficient. Note that this form of the gamma density has been divided by the value at the mode such that the maximum value is always 1.0. The dispersion coefficient K is allow to change linearly with age or length (i.e., $K=\kappa+\gamma a$ or $K=\kappa+\gamma l$)

The logistic function was used to model the relationship between p and l or a . In addition, the possible effect of depth (d), gear type (g ; vertical line or longline), region (r ; east or west of the Mississippi River) were incorporated such that

$$(5) \quad \begin{cases} p(a, d, r, g) = \lambda^r \pi_g / (1 + e^{\alpha_g + \chi r + \delta d + \beta_g a}) \\ p(l, d, r, g) = \lambda^r \pi_g / (1 + e^{\alpha_g + \chi r + \delta d + \beta_g l}) \end{cases}$$

π_g = maximum attainable spawning proportion (absent a gear effect, $\pi_g = \pi$)

α_g = inflection point of logistic function (absent a gear effect, $\alpha_g = \alpha$)

β_g = slope of logistic function of age or length (absent a gear effect, $\beta_g = \beta$)

λ = effect of region on maximum spawning proportion ($r = 0$ for west, 1 otherwise)

χ = effect of region on inflection point of logistic function ($r = 0$ for west, 1 otherwise)

δ = slope of logistic function of depth

The observations of spawning condition are based on the presence or absence of spawning markers. A value of 1 is assigned if spawning markers are present and a value of 0 if they are not. Accordingly, the parameters of the model for $p(a, l, d, r, g, t)$ defined in equations 3-5 may be estimated by a nonlinear Bernoulli regression, i.e., by minimizing the negative loglikelihood expression

$$(6) \quad -\ln L = -\sum_i^N o_i \ln(p_i) + (1 - o_i) \ln(1 - p_i)$$

where i denotes one of N observations, o_i is the observed presence (1) or absence (0) of a spawning marker in sample i , and p_i is the probability of observing a spawning marker predicted by equation 3 given the values of the covariates a , l , d , g , or r associated with sample i . The numerical minimization of (6) was accomplished using Excel Solver and AD Model Builder.

Statistical comparisons

Statistical comparisons among alternative models were made using Akaike's information criterion (AIC; Akaike 1973):

$$\text{AIC} = -2\ln L + 2n ,$$

where n is the total number of parameters estimated and L is the measure of goodness of fit (e.g., likelihood function) being maximized. The AIC attempts to identify the most parsimonious explanation of the data by balancing the relative improvement in model fit against the number of parameters required to achieve that fit. The 'best' model is considered to be the one with the lowest AIC. A rule of thumb is that differences in AIC (Δ) of less than 2 constitute weak evidence that one model is better than another, differences between 3 and 10 are regarded as moderate evidence, and differences greater than 10 are regarded as strong evidence (Burnham and Anderson 2002). A pseudo R^2 statistic was also computed as the fraction of the variance explained by the regression:

$$R^2 = 100\% \left(1 - \frac{\sum_i^N (o_i - \hat{p}_i)^2}{\sum_i^N (o_i - \bar{o})^2} \right)$$

where \bar{o} is the simple mean of the observations and \hat{p} is the maximum likelihood estimate of the probability that a fish will have spawning markers.

Conversion to total number of eggs produced

The average spawning fraction during the course of a year for age or length x is obtained as

$$(7) \quad \bar{p}(x) = p(x) \int_{t=0}^1 p(t|x) dt .$$

In cases where $p(t|a)$ and $p(t|l)$ are estimated to be essentially 0 at $t=1$,

$$(8) \quad \int_{t=0}^1 p(t|x) dt \cong \int_{t=0}^{\infty} p(t|x) dt = \frac{\Gamma(\phi) \kappa^\phi}{(\mu/e)^{\phi-1}}$$

where the right hand side of (8) is simply the inverse of the gamma density evaluated at the mode. In cases where spawning occurs throughout the year, the integral in (7) must be evaluated numerically.

The prevalence of hydrated oocytes and postovulatory follicles (histological spawning markers) can be detected over a period of about 34 hours (see Fitzhugh et al. 2012). Following Priede and Watson (1993), the average spawning fraction can be converted to a daily probability of spawning P :

$$(9) \quad \bar{P}(x) = \frac{24}{T_M} \bar{p}(x)$$

where T_M is the duration in hours (here 34) that spawning markers can be detected. The expected number of spawns during the course of a year is therefore obtained from multiplying (9) by the number of days, i.e.,

$$(10) \quad s(x) = 365 \frac{24}{34} \frac{\Gamma(\phi) \kappa^\phi}{(\mu/e)^{\phi-1}}.$$

The total number of eggs produced during the spawning season (E) is

$$(11) \quad E(x) = s(x)BF(x).$$

Results

Batch fecundity

Plots of red snapper BF against total length and age are shown in Figures 1a and 1b, respectively. Fecundity appears to increase geometrically with length and more or less asymptotically with age. The addition of the 85 new records did not substantially change the apparent relationship between BF and age or length. The updated equations are

$$(12) \quad BF(a) = 1.732(1 - e^{-0.29a})^{6.047}$$

$$(13) \quad BF = 1.449E - 08l^{4.196}$$

Note that, in the case of equation (13), the multiplicative parameter (c in equation 1) has been adjusted by the lognormal bias-correction factor ($e^{\sigma^2/2}$).

Spawning fraction

Stepwise model building exercises were developed beginning with the null model ($p=\pi$), which assumes all fish have the same probability of being found in spawning condition. In the first step, the logistic age or length effects were added to the null model. The corresponding AIC values were decreased by more than 40 and about 6% of the residual variance was explained (Table 1). Accordingly, the statistical evidence for both the age and length effects was strong and these terms were retained in all subsequent models.

In the second step, spawning fraction was allowed to vary with time of year to accommodate the limited duration of the spawning season. Initially, the duration of the spawning season duration was assumed to be independent of age or length (i.e., $\gamma = 0$). In that case the AIC values were further reduced by over 200 and about 30% of the residual variance was explained. Accordingly, the statistical evidence for a seasonal effect on spawning fraction was strong and these terms were retained in all subsequent models.

In the third step, the potential variation in season duration with age or length was investigated by estimating the parameter γ . The resulting AIC values suggested little evidence for a variation in season duration with age ($\Delta < 3$) and only moderate evidence for a variation in season duration with length ($\Delta < 10$). Moreover, the percentage of variation explained by the model was negligibly improved.

Finally, the effects of incorporating the covariates depth, gear and region were examined by adding the corresponding parameters to the seasonal model derived from step 2 (one covariate at a time). The model fits suggested little evidence for a gear and regional effects ($\Delta < 3$), but strong evidence for a depth effect ($\Delta > 10$). None of these models, however, contributed to explaining a substantial fraction of the variance. Even the full model incorporating all parameters did not substantially improve the explanatory power of the regression (Figure 2). For the length based analysis, the R^2 for the full model was 33% compared to 30% for the length+season model. For the age-based analysis, the R^2 for the full model was 31% compared to 29% for the age+season model. Accordingly, the final model included only age or length and time of year.

The spawning season was estimated to occur primarily from early April to early November, with a peak in July (Figure 3). Spawning fraction was estimated to increase rapidly with length or age, starting at very low values for fish under 300 mm (age 1) and

beginning to level off around 500 mm (age 6-7). There were no obvious trends in the residuals (difference between model fit and observed data) to suggest that the model was not fitting the oldest (or youngest) age classes (Figure 2). The asymptotic estimates of the variance of the parameters and associated correlation matrix (obtained from the Hessian via the application in AD Model Builder) are shown in Table 2.

Conversion to total number of eggs produced

The estimates of spawning fraction at age from the final models discussed above were converted to the daily probability of spawning (P), total number of spawns per year (s) and total number of eggs produced following equations 9-11. The results from the length-based models are summarized in Table 3 and Figure 4. The results from the age-based models are summarized in Table 4 and Figure 5.

Discussion

Previous assessments of Gulf of Mexico red snapper characterized the relative fecundity of different age classes by multiplying estimates of the batch fecundity at age by estimates of the maturity at age. The new estimates of batch fecundity obtained with the 85 additional records were very similar to those used in previous assessments, being only slightly lower in magnitude and almost identical in relative trend. The new estimates of daily spawning fraction suggest that red snapper less than 6 years old contribute considerably less to the spawning population than was indicated by the maturity data, suggesting that even when mature, younger fish spawn less frequently than older fish. However, the low batch fecundity values estimated for the younger age classes mitigate the importance of these differences to the estimation of per capita egg production; the estimated relative per capita egg production at age being rather similar to that used in previous assessments.

Acknowledgments

Thanks are due to Melissa Cook and the EASA sampling team at the NMFS Pascagoula Laboratory conducting the field sampling. Erik Lang oversaw the reproductive data collection and processing and conducted the quality control assessment.

Beverly Barnett and Hanna Lang organized and proofed the data from all the biological collections. Hope Lyon conducted the histological readings. Robert Allman and the NMFS Panama City aging team provided the age data.

Literature cited

Akaike, M. 1973. Information theory and an extension of the maximum likelihood principle. In B. Petrov and F. Csaki, eds., Proc. 2d International Symposium on Information Theory, pp. 267-281. Budapest, Hungary: Akademia Kiado.

Brown-Peterson, N., K. M. Burns, and R. M. Overstreet. 2009. Regional differences in Florida red snapper reproduction. Proceedings of the Gulf and Caribbean Fisheries Institute 61:149-155.

Burnham, K.P. and D.R. Anderson 2002. Model selection and Multimodal Inference: A Practical Information-Theoretic Approach, 2nd Edition. Springer-Verlag, New York.

Campbell, M., T., A. Pollack, T. Henwood., J. Provaznik and M. Cook. 2012. Summary report of the red snapper (*Lutjanus campechanus*) catch during the 2011 expanded annual stock assessment (EASA). Mississippi Laboratories. SEDAR31-DW-17. 27 p.

Cooper, W.T., L.R. Barbieri, M.D. Murphy and S.K. Lowerre-Barbieri. 2013. Assessing reproductive potential in species with indeterminate fecundity: Effects of age truncation and size-dependent reproductive timing. Fisheries Research 138:31-41.

Cowan, J. H., K. M. Boswell, K. A. Simonsen, C. R. Saari, and D. Kulaw. 2012. SEDAR31-DW03 Working paper for red snapper data workshop SEDAR 31. Louisiana State University, Baton Rouge, Louisiana.

Fitzhugh, G.R., K.W. Shertzer, G.T. Kellison and D.M. Wyanski. 2011. Review of size- and age-dependence in batch spawning: implications for stock assessment of fish species exhibiting indeterminate fecundity. Fish Bull. 110:413-425.

Fitzhugh, G.R., E.T. Lang, and H. Lyon. 2012. Expanded Annual Stock Assessment Survey 2011: Red Snapper Reproduction. Panama City Laboratory Contribution Series 12-05. Working Document, SEDAR 31-DW-07-. 31 p.

Kulaw, D. 2012. Habitat- and region-specific reproductive biology of female red snapper (*Lutjanus campechanus*) in the Gulf of Mexico. MS Thesis. Louisiana State University. 165 p.

Klibansky, N., and F. Juanes. 2008. Procedures for efficiently producing high-quality fecundity data on a small budget. *Fisheries Research* 89:84-89.

LaPlante, L. H., and E. T. Schultz. 2007. Annual fecundity of tautog in Long Island Sound: size effects and long-term changes in a harvested population. *Trans. Am. Fish. Soc.* 136:1520–1533.

Lowerre-Barbieri, S.K., K. Ganas, F. Saborido-Rey, H. Murua, and J.R. Hunter. 2011. Reproductive timing in marine fishes: variability, temporal scales, and methods. *Mar. Coast. Fish.* 3:71-91.

Lowerre-Barbieri, S.K., N. J. Brown-Peterson, H. Murua, J. Tomkiewicz, D.M. Wyanski, and F. Saborido-Rey. 2011. Emerging issues and methodological advances in fisheries reproductive biology. *Mar. Coast. Fish.* 3:32-51

Mehault, S., R. Dominguez-Petit, S. Cervino and F. Saborido-Rey. 2010. Variability in total egg production and implications for management of the southern stock of European hake. *Fisheries Research* 104:111-122.

Porch, C. E. 2004. Batch-fecundity and maturity estimates for the 2004 assessment of red snapper in the Gulf of Mexico. Working Document SEDAR7-AW-5 (Revised). 17 pp.

Porch, C.E., G.R. Fitzhugh, M.S. Duncan, L.A. Collins, and M.W. Jackson. 2007. Modeling the dependence of batch fecundity on size and age for use in stock assessments of red snapper in U.S. Gulf of Mexico waters. Pages 229-244 in: W.F. Patterson, III, J. H. Cowan, Jr., G.R. Fitzhugh, and D.L. Nieland, editors. Red snapper ecology and fisheries in the U.S. Gulf of Mexico. American Fisheries Society, Symposium 60, Bethesda Maryland.

Priede, I.G. and J.J. Watson. 1993. An evaluation of the daily egg production method for estimating biomass of Atlantic mackerel (*Scomber scombrus*). Bull. Mar. Sci. 53(2):891-911.

Szedlmayer, S. T., and C. Furman. 2000. Estimation of abundance, mortality, fecundity, age frequency, and growth rates of red snapper, *Lutjanus campechanus*, from a fishery-independent stratified random survey. Report to the Gulf and South Atlantic Fisheries Foundation, Inc. National Oceanographic and Atmospheric Administration, Department of Commerce Cooperative agreement NA87FM0221.

Table 1. Selected models for red snapper spawning fractions developed during the stepwise model building procedure (based on the Bernoulli regression of equation 5). The shaded region highlights the final models. The use of t' indicates the model allows the seasonal effect to vary with age or length.

Length-based models

Statistic	p	$p(l)$	$p(l,t)$	$p(l,t')$	$p(l,t,d)$	$p(l,t,g)$	$p(l,t,r)$	$p(l,t',d,r,g)$
π	0.3904	0.5465	0.8660	0.8581	0.8862	0.8907	0.8628	0.8725
α		3.2945	9.0840	12.7602	6.3114	-6.0841	5.2228	-6.0829
β		-0.0794	-0.2723	-0.4185	-0.2504	-0.6425	-0.1516	-0.6421
μ			0.5363	0.5347	0.5371	0.5386	0.5407	0.5401
κ			0.0244	0.0031	0.0249	0.0259	0.0244	0.0144
γ				0.0004				0.0002
δ_D					0.4738			0.7255
λ							1.1963	1.1694
χ							-0.3508	-0.2935
π_G						0.7731		0.8167
α_G						9.7794		7.2529
β_G						-0.2994		-0.3146
<i>AIC</i>	1339	1283	1000	992	986	1004	998	981
r^2	NA	6	30	31	32	30	31	33

Age-based models

Statistic	p	$p(a)$	$p(a,t)$	$p(a,t')$	$p(a,t,d)$	$p(a,t,g)$	$p(a,t,r)$	$p(a,t',d,r,g)$
π	0.3881	0.5635	0.9399	0.8776	0.9203	0.9345	0.9481	0.8738
α		1.8891	1.6962	1.5473	1.1703	0.2223	1.9391	0.9122
β		-0.5134	-0.6504	-0.8613	-1.0550	-0.4906	-0.6123	-2.0861
μ			0.5381	0.5354	0.5375	0.5390	0.5420	0.5391
κ			0.0255	0.0123	0.0251	0.0262	0.0254	0.0142
γ				0.0020				0.0016
δ_D					0.3297			0.4117
λ							1.0960	1.1812
χ							-1.3479	-0.5065
π_G						0.8958		0.9102
α_G						1.6529		-0.1621
β_G						-0.6355		-0.8530
<i>AIC</i>	1327	1283	1008	1007	995	1011	998	994
r^2	NA	5	29	29	30	29	30	31

Table 2. Correlation matrix for final models.

Statistic	Estimate	Std. error	Correlation coefficients				
			π	α	β	γ	κ
Length-based model							
π	0.8660	0.0315	1.0				
α	-0.2723	0.1086	0.2	1.0			
β	9.0840	3.5484	-0.2	-1.0	1.0		
μ	0.5363	0.0048	-0.3	0.2	-0.2	1.0	
κ	0.0244	0.0019	-0.5	0.2	-0.2	0.2	1.0
Age-based model							
π	0.9399	0.0409	1.0				
α	-0.6504	0.1740	0.6	1.0			
β	1.6962	0.6135	-0.4	-0.9	1.0		
μ	0.5381	0.0050	0.0	0.1	0.0	1.0	
κ	0.0255	0.0019	-0.1	0.1	0.1	0.1	1.0

Table 3. Predicted spawning fraction at peak season p , daily spawning fraction P , average daily spawning fraction over the course of the year \bar{P} , total number of spawns per year s , batch fecundity BF (in millions), total number of eggs produced E (in millions), and relative fecundity ($E(l)/\text{MAX}_l E(l)$).

TL(cm)	$p(l)$	$P(l)$	$\bar{P}(l)$	$s(l)$	$BF(l)$	$E(l)$	Rel $E(l)$
10	0.000	0.000	0.000	0	0.000	0.00	0.000
12	0.000	0.000	0.000	0	0.000	0.00	0.000
14	0.004	0.003	0.001	0	0.001	0.00	0.000
16	0.008	0.005	0.002	1	0.002	0.00	0.000
18	0.013	0.009	0.003	1	0.003	0.00	0.000
20	0.022	0.016	0.005	2	0.004	0.01	0.000
22	0.038	0.027	0.008	3	0.006	0.02	0.000
24	0.063	0.044	0.013	5	0.009	0.04	0.000
26	0.103	0.073	0.021	8	0.013	0.10	0.001
28	0.163	0.115	0.033	12	0.017	0.21	0.001
30	0.248	0.175	0.050	18	0.023	0.42	0.003
32	0.354	0.250	0.072	26	0.030	0.79	0.005
34	0.471	0.332	0.096	35	0.039	1.35	0.009
36	0.582	0.411	0.118	43	0.049	2.13	0.014
38	0.675	0.477	0.137	50	0.062	3.09	0.021
40	0.744	0.525	0.151	55	0.077	4.22	0.029
42	0.791	0.558	0.161	59	0.094	5.51	0.037
44	0.821	0.579	0.167	61	0.114	6.95	0.047
46	0.839	0.592	0.170	62	0.138	8.57	0.058
48	0.850	0.600	0.173	63	0.165	10.38	0.070
50	0.857	0.605	0.174	64	0.195	12.41	0.084
52	0.861	0.608	0.175	64	0.230	14.69	0.099
54	0.863	0.609	0.175	64	0.270	17.26	0.117
56	0.864	0.610	0.176	64	0.314	20.14	0.136
58	0.865	0.611	0.176	64	0.364	23.35	0.158
60	0.865	0.611	0.176	64	0.420	26.94	0.182
62	0.866	0.611	0.176	64	0.482	30.92	0.209
64	0.866	0.611	0.176	64	0.550	35.33	0.239
66	0.866	0.611	0.176	64	0.626	40.21	0.272
68	0.866	0.611	0.176	64	0.710	45.58	0.308
70	0.866	0.611	0.176	64	0.802	51.47	0.348
72	0.866	0.611	0.176	64	0.902	57.93	0.392
74	0.866	0.611	0.176	64	1.012	64.99	0.440
76	0.866	0.611	0.176	64	1.132	72.69	0.492
78	0.866	0.611	0.176	64	1.263	81.06	0.549
80	0.866	0.611	0.176	64	1.404	90.15	0.610
82	0.866	0.611	0.176	64	1.557	99.99	0.677
84	0.866	0.611	0.176	64	1.723	110.63	0.749
86	0.866	0.611	0.176	64	1.902	122.12	0.826
88	0.866	0.611	0.176	64	2.094	134.48	0.910
90	0.866	0.611	0.176	64	2.302	147.78	1.000

Table 4. Predicted spawning fraction at peak season p , daily spawning fraction P , average daily spawning fraction over the course of the year \bar{P} , total number of spawns per year s , batch fecundity BF (in millions), total number of eggs produced E (in millions), and relative fecundity ($E(a)/\text{MAX}_a E(a)$).

Age	$p(a)$	$P(a)$	$\bar{P}(a)$	$s(a)$	$BF(a)$	$E(a)$	Rel $E(a)$
0	0.000	0.000	0.000	0	0.000	0.00	0.000
1	0.000	0.000	0.000	0	0.000	0.00	0.000
2	0.378	0.267	0.079	29	0.012	0.35	0.003
3	0.530	0.374	0.110	40	0.065	2.62	0.021
4	0.669	0.472	0.139	51	0.178	9.07	0.073
5	0.776	0.548	0.162	59	0.344	20.30	0.164
6	0.847	0.598	0.176	64	0.540	34.71	0.281
7	0.889	0.627	0.185	68	0.740	49.95	0.404
8	0.913	0.644	0.190	69	0.927	64.27	0.520
9	0.925	0.653	0.193	70	1.092	76.76	0.621
10	0.932	0.658	0.194	71	1.231	87.15	0.705
11	0.936	0.661	0.195	71	1.344	95.53	0.773
12	0.938	0.662	0.195	71	1.434	102.15	0.826
13	0.939	0.663	0.195	71	1.505	107.30	0.868
14	0.939	0.663	0.195	71	1.559	111.27	0.900
15	0.940	0.663	0.196	71	1.601	114.30	0.924
16	0.940	0.663	0.196	71	1.634	116.61	0.943
17	0.940	0.663	0.196	71	1.658	118.36	0.957
18	0.940	0.663	0.196	71	1.676	119.68	0.968
19	0.940	0.663	0.196	71	1.690	120.67	0.976
20	0.940	0.663	0.196	71	1.701	121.42	0.982
21	0.940	0.663	0.196	71	1.709	121.98	0.986
22	0.940	0.663	0.196	71	1.714	122.40	0.990
23	0.940	0.663	0.196	71	1.719	122.72	0.992
24	0.940	0.663	0.196	71	1.722	122.96	0.994
25	0.940	0.663	0.196	71	1.725	123.13	0.996
26	0.940	0.663	0.196	71	1.726	123.27	0.997
27	0.940	0.663	0.196	71	1.728	123.37	0.998
28	0.940	0.663	0.196	71	1.729	123.44	0.998
29	0.940	0.663	0.196	71	1.730	123.50	0.999
30	0.940	0.663	0.196	71	1.730	123.54	0.999
31	0.940	0.663	0.196	71	1.731	123.57	0.999
32	0.940	0.663	0.196	71	1.731	123.59	0.999
33	0.940	0.663	0.196	71	1.731	123.61	1.000
34	0.940	0.663	0.196	71	1.731	123.62	1.000
35	0.940	0.663	0.196	71	1.732	123.63	1.000
36	0.940	0.663	0.196	71	1.732	123.64	1.000
37	0.940	0.663	0.196	71	1.732	123.65	1.000
38	0.940	0.663	0.196	71	1.732	123.65	1.000
39	0.940	0.663	0.196	71	1.732	123.65	1.000
40	0.940	0.663	0.196	71	1.732	123.65	1.000

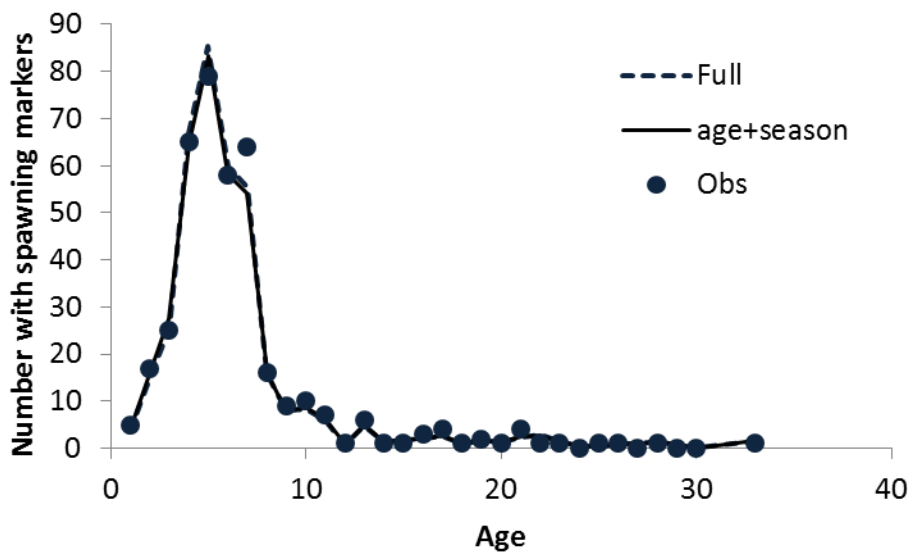
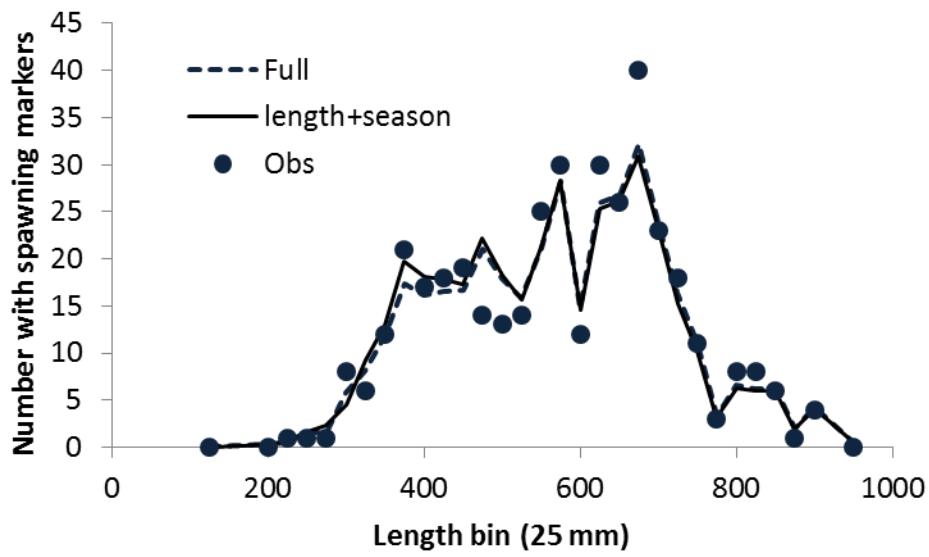


Figure 2. Observed number of red snapper with spawning markers compared with the corresponding predictions the final model (age or length + season) and full model (all covariates included).

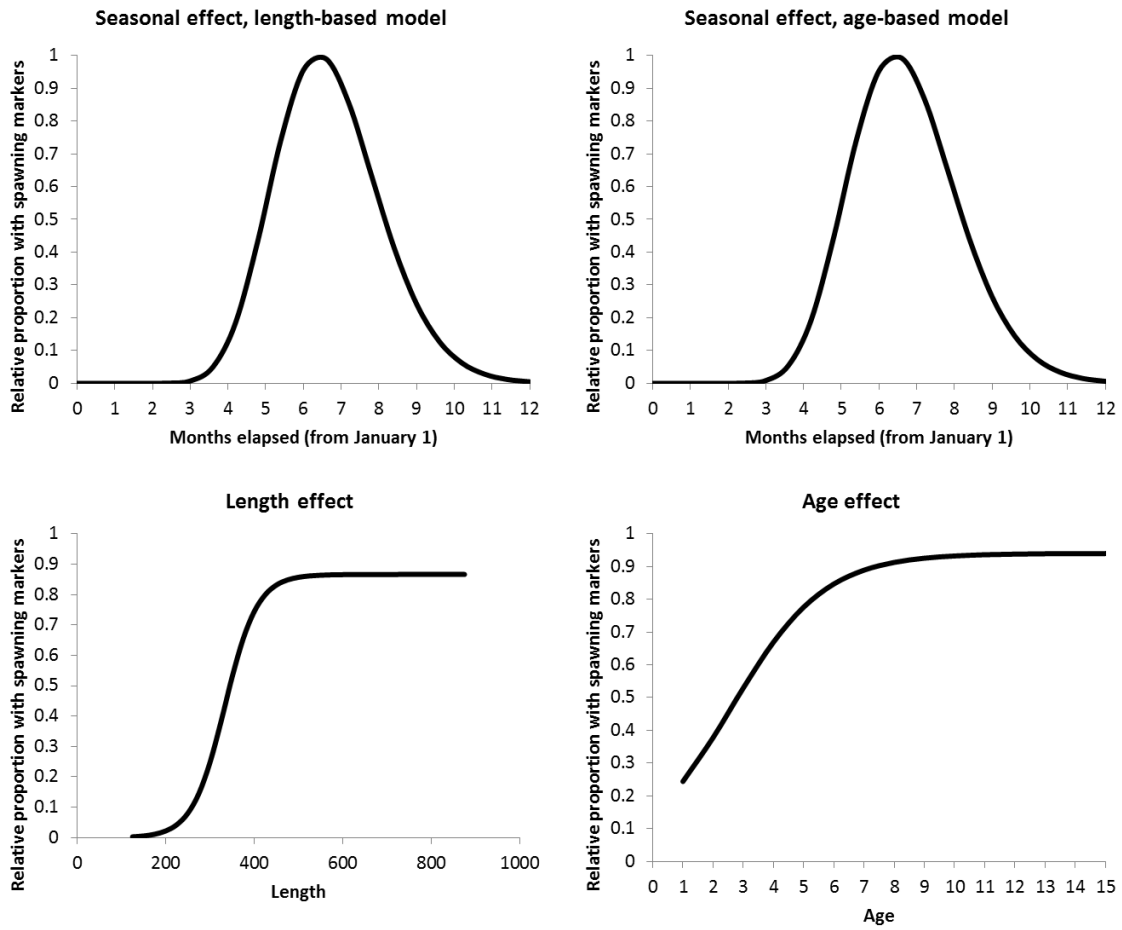


Figure 2. Predicted relationships between spawning fraction and age, length, and time of year.

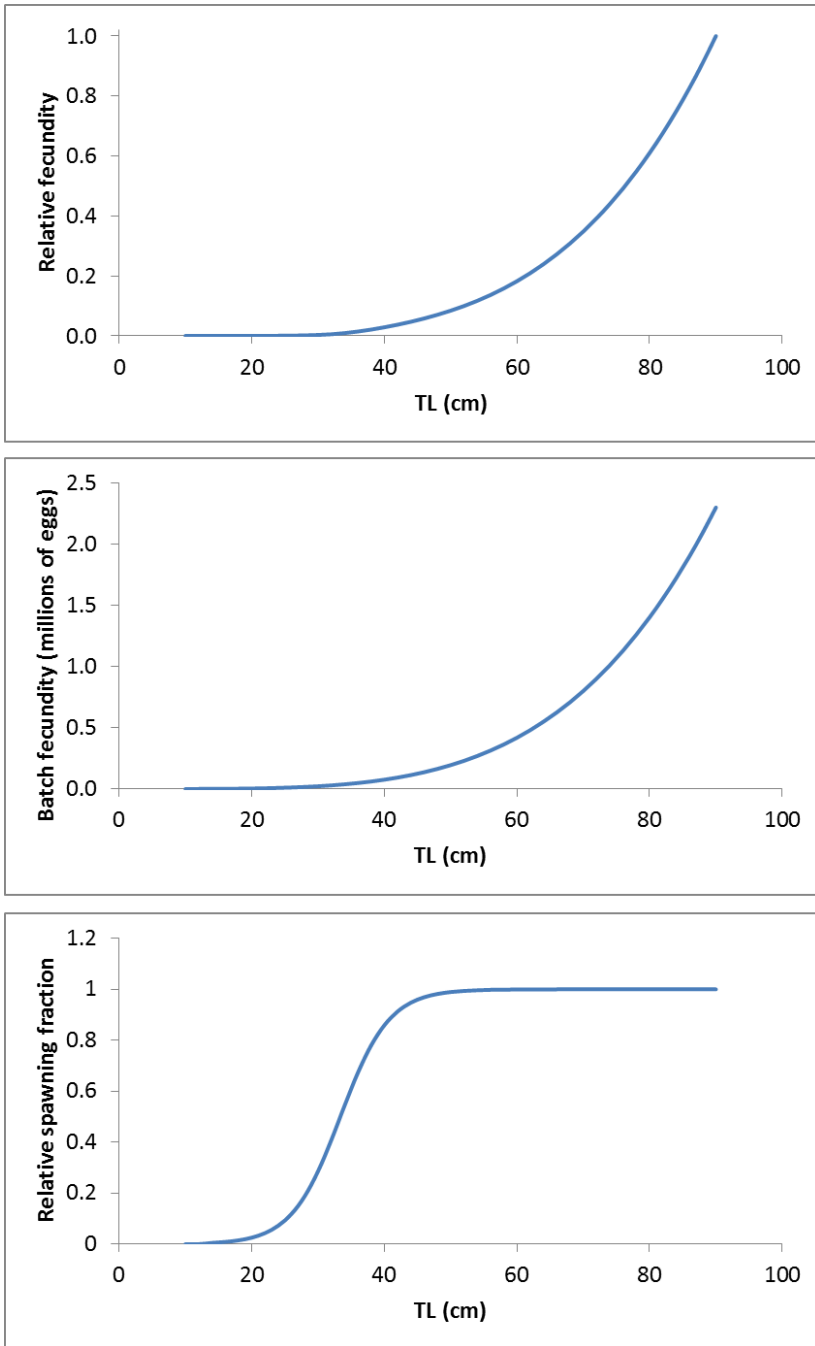


Figure 3. Plots of length-based predictions of relative fecundity at age, batch fecundity at age, and the relative spawning fraction.

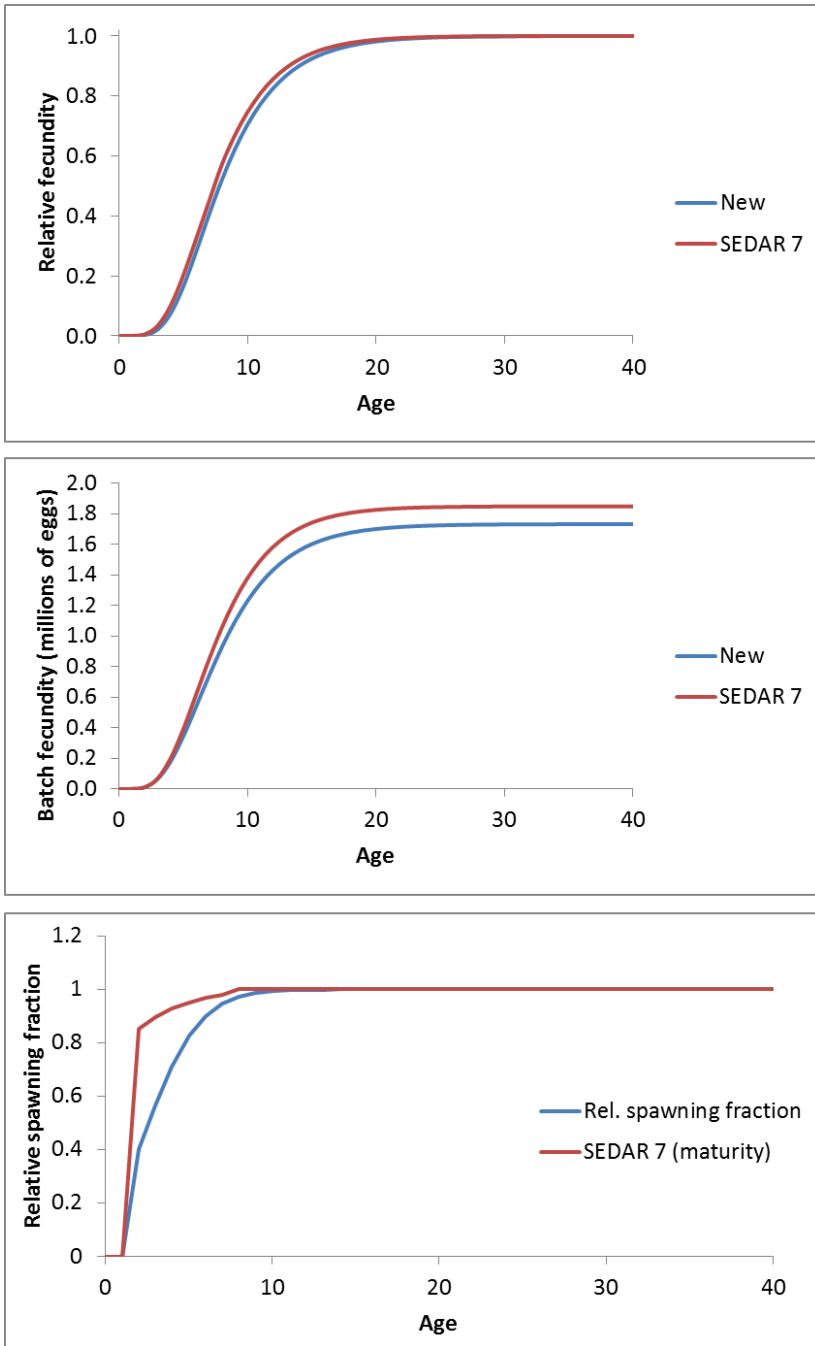


Figure 4. Plots of age-based predictions of relative fecundity at age, batch fecundity at age, and the relative spawning fraction. Comparison is made with the vectors used during SEDAR 7 and subsequent updates.